Journal of Alloys and Compounds, 194 (1993) 245–249
JALCOM 7216

Nanophase processing of amorphous alloys*

L. S. Kim, H. Chang and R. S. Averback
Department of Materials Science and Engineering, University of Illinois at Urbana-Champaign Urbana, IL 61801 (USA)

(Received February 10, 1992; in final form June 5, 1992)

Abstract

Since the pioneering work on the formation of amorphous alloys by Duwez and coworkers using rapid quenching, a number of different strategies for producing metallic glasses have emerged. However, the problem of processing bulk amorphous alloys remains an elusive goal. We have been exploring the possibilities of using a nanophase ultrafine amorphous particles, of approximately 5 nm, that can be compacted into bulk forms *in situ*. We have used both joule heating and magnetron sputtering methods to synthesize amorphous alloys of Ni–Ti, Ni–Tb, Pd–Y, and Ti–1Al. These alloys were characterized by X-ray diffraction and differential scanning calorimetry. Preliminary results on sintering, crystallization, and mechanical properties of these nanophase materials are discussed.

1. Introduction

Amorphous alloys have a number of attractive properties for technological applications: corrosion and oxidation resistance, high strength, and high magnetic permeabilities and electrical resistances. However, owing to the difficulty in synthesizing and processing these materials, they have presently found only limited usage. Much of the problem derives from the metastable structure of amorphous alloys, since it tends toward the more stable crystalline state upon heating. The most common commercial procedure for producing these alloys is rapid quenching, but due to the natural limitation of heat removal, only thin strips can be produced. Consolidation of bulk components is also difficult since heat treatment again results in crystallization. Recently, other methods, such as the solid state amorphizing transformation (SSAT) [1], ball milling [2], or rolling [3] seem promising, although they too are strongly limited by dimensionality considerations: SSAT requires diffusion through the growing amorphous phase to effect the crystalline to amorphous transformation, while ball milling requires diffusion for sintering of the micron-sized particles. A natural solution to this problem is to reduce the length scale over which the diffusion must take place to fully synthesize and process the amorphous alloy. Similar difficulties arise in the processing of ceramic materials where grain growth rather than crystallization during sintering and heat treatments must be avoided. Nanophase processing has shown to be a very promising method in these materials (see, for example, ref. 4) and it is reasonable to suspect that it may also be useful for processing bulk amorphous alloys.

Nanophase processing refers to the synthesis of powders with ultra-fine particle size and their subsequent consolidation and forming [5]. The advantage of nanophase processing for fabricating materials that are thermodynamically unstable is that the length scale over which diffusion must take place for sintering or deformation is very small; thus the processing temperatures can be kept low, so that the flow of the system toward equilibrium can be kinetically restricted. The reduction in the temperature required for densification can be seen from the expression [6],

$$\partial\rho/\partial t = \gamma_s\Omega/kT[F_v(\rho)D_v/d^3 + F_b(\rho)D_b\delta_b/d^4] \quad (1)$$

where ρ is the density, γ_s is the surface energy, Ω is the atomic volume, D_v and D_b are the diffusion coefficients in the bulk and grain boundaries, respectively, δ_b is the grain boundary width, $F_i(\rho)$ are functions of density and d is the grain size. Because of its dependence on d^{-4}, the densification of powders that have particles on the nanometer rather than micrometer scale can occur at a rate 12 orders of magnitude more rapid and hopefully providing the necessary processing window for densification without crystallization.

An important assumption of eqn. (1) is that the interparticle contacts behave as grain boundaries in that the centers of the particles approach one another during sintering by atoms (vacancies) flowing from

*Paper presented at the Symposium on Solid State Amorphizing Transformations, TMS Fall Meeting, Cincinnati, OH, October 21–24, 1991.

0925-8388/93/$6.00

sources in the grain boundaries (pores) to sinks in the pores (grain boundaries). Pores are not voids within the bulk material; removal of voids is generally a much higher temperature process. A fundamental question for the sintering of amorphous alloys, therefore, is whether grain boundaries, or interparticle boundaries, defined in this way can exist for amorphous alloys, or whether interparticle boundaries become diffuse before sintering can take place. In other words, do the interparticle contacts in nanophase amorphous compacts provide sources and sinks for atoms and free volume?

A second question that must be addressed is whether the inert gas condensation is conducive to forming amorphous particles. Previous work on the metal–metalloid systems, Au–Si and Pd–Si–Fe [7, 8] and on one metal–metal (NiTi) [9] indicate that it is, although these systems are certainly some of easiest glass forming systems available, and additional work is necessary to explore the process. Furthermore, no attempt was made in these first studies to examine the sinterability or stability of the alloys.

2. Experimental details

The nanophase processing system employed for these studies is essentially the same as that described by Birringer *et al.* [10]. The important feature of this system for the production of amorphous alloys is that the particles are formed by the condensation of hot metal vapor in a cold inert gas. For nonequilibrium processing of alloys, the time–temperature history of the particles is of fundamental importance. Although no study of this type was performed here, the time–temperature history of particles produced by a similar means was considered by Yatsuya *et al.* [11]. They estimated that once the particles attained their maximum size in the growth zone above the evaporation source, they quickly came into thermal equilibrium with the inert gas. They also measured the velocity and temperature gradient of the convection current of the gas above the source; these were 100 cm s^{-1} and 200 K cm^{-1}, respectively. Consequently, the cooling rate of the nanophase particles is approximately 2×10^4 K s^{-1}. Although faster rates are possible by other rapid quenching systems, this rate is sufficient for quenching in the amorphous phase in many systems. In addition, the small size and separation of the particles requires that nucleation take place in most of the particles since growth processes cannot much influence the volume fraction of crystalline material. It is noteworthy that Yatsuya *et al.* attempted to synthesize amorphous Pd–Si particles by this method but without success [11].

A final consideration for synthesizing alloy particles by direct evaporation of a bulk alloy is the control of the composition and homogeneity of the particles. In rather few alloy systems are the partial vapor pressures of the components above the liquid alloy equal. The early work cited above made little attempt to control the alloy composition of the particles and perhaps this prevented Yatsuya from obtaining amorphous particles. The different vapor pressures of the alloy components raises two problems: the nanophase particles have different compositions than the bulk alloy, and the composition of the particles changes as the bulk alloy changes its composition. In the present work, this problem was addressed by choosing alloy systems and compositions where the relative vapor pressures of the components over the alloy were equal to their relative concentration in the liquid alloy. The alloy composition was selected, therefore, using eqn. (2) as a guide; it relates the ratio of the vapor pressures of the alloy components to their molar fraction in the alloy, X_i, the vapor pressures of the pure components and the heat of mixing parameter, Ω. Equation (2) was derived using a regular solution model:

$$\frac{p_A}{p_B} = \frac{\{X_A p_A^0\}}{\{X_B p_B^0\}} \exp\left\{\frac{\Omega}{RT}(X_B - X_S)\right\} \tag{2}$$

Examination of eqn. (2) shows that for any alloy system, there is one alloy composition where the ratio of the vapor pressures of the components over the alloy is equal to the ratio of their molar fractions. At this alloy concentration, the evaporation is stable. Unfortunately, the stable concentration is fixed by the alloy system and not adjustable. For this reason, alloy systems were selected in this study according to their known or suspected facility for quenching into the glassy state at the stable concentration.

3. Results

Four alloy systems were investigated in this study. They are listed in Table 1 along with relevant thermodynamic data. The compositions of the nanophase amorphous alloys were determined by Rutherford backscattering analysis. These systems all are comprised of binary early transition–late transition metals, which have large (negative) heats of mixing and are readily evaporated from a tungsten boat. X-ray diffraction was the

TABLE 1. Four alloy systems investigated with their synthesized compositions and relevant thermodynamic data

Alloy	Composition	Ω (kJ mol^{-1})	P_A^0/P_B^0
NiTi	50:50	−160	33
NiTb	50:50	−110[a]	6.7×10^{-1}
PdY	40:60	−332	50
TiAl[b]	42:58	−119	9.3×10^{-4}

[a]Estimated.
[b]Prepared by sputtering.

principal method for determining whether the consolidated nanophase alloy was amorphous. Diffraction patterns for the different alloys are illustrated in Figs. 1(a)–(c) and Fig. 2. Although the broad peaks seen in these diffraction patterns are characteristic of those obtained from amorphous material, broad peaks are not, in general, definitive in proving that the alloys are amorphous [12]. Line widths also are broad when the grain size is extremely small. For the grain sizes typical of this processing method which are larger than 4 nm, this concern is probably unwarranted. The diffraction pattern for the TiAl sample, Fig. 2, indicates that this alloy was partially crystalline in the as-compacted state, as indicated by the sharper (200) reflection. This alloy, unlike the others, was synthesized by sputtering rather than boat evaporation. The evolution of the structure of the TiAl sample as a function of annealing treatment is also shown in Fig. 2. After annealing at 250 °C, the grain size was found to be 10 nm. The properties of this nanophase intermetallic alloy will be published elsewhere [13]. The diffraction pattern for the PdY also appears unusual. We suspect that large composition fluctuations present in the sample give rise to the very broad diffraction peak which appears to show broad subpeaks.

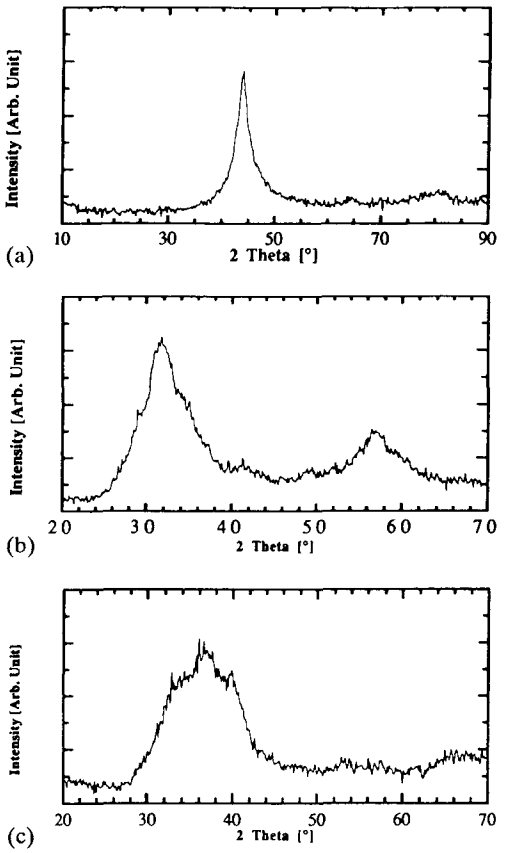

Fig. 1. X-ray diffraction patterns for the different alloys showing the broad peaks from amorphous phases: (a) NiTi compacted at 150 °C; (b) NiTb compacted at 150 °C; (c) PdY compacted at RT.

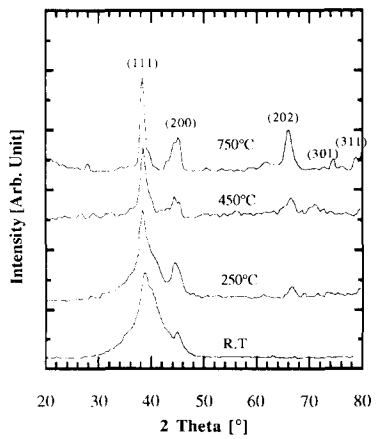

Fig. 2. X-ray diffraction patterns for the TiAl at different annealing stages.

Differential scanning calorimetry (DSC) measurements were also performed on these samples as shown in Figs. 3(a)–(d). For only two alloys could the complete heat evolution be followed, NiTi and TiAl; release of excess enthalpy in the other systems was continuing at temperatures above the measuring capability of the DSC instrument. The two noteworthy results obtained from these measurements are the large enthalpy change, 20–40 kJ mol^{-1}, and the broad range of temperatures at which the release takes place. The enthalpy of crystallization is typically 5–10 kJ mol^{-1} and generally occurs over a narrow temperature interval in DSC scans. However, Jang and Koch have reported similar large enthalpies for the crystallization of amorphous Ni_3Al produced by ball milling. Clearly other sources of enthalpy are available during the heat treatment. Possible candidates, in addition to the crystallization enthalpy, are (i) grain boundaries, (ii) pore surfaces, (iii) atomic ordering. We now estimate their magnitudes.

The contributions from the elimination of grain boundaries and pores can be estimated by assuming that the consolidated amorphous alloy is comprised of cubic grains with sides of length, d, so that the enthalpy stored in the grain boundaries is,

$$\Delta H = \frac{3\gamma_b \bar{V}}{d} \tag{3}$$

where $\bar{V}$ is the molar volume and γ_b is the grain boundary energy. With a value $\gamma_b = 1.5$ J m^{-2}, eqn. (3) yields 10 kJ mol^{-1}. This estimate for the grain boundary enthalpy is in agreement with that observed by Hellstern *et al.* for ball-milled Ru [2]. If it is further assumed that consolidated material has approximately 5%–15% porosity (see below), and that the surface energy is 2 J m^{-2}, another 5 kJ mol^{-1}, or 15 kJ mol^{-1} is available from these sources. The enthalpy derived from ordering reactions is more difficult to estimate, since the degree

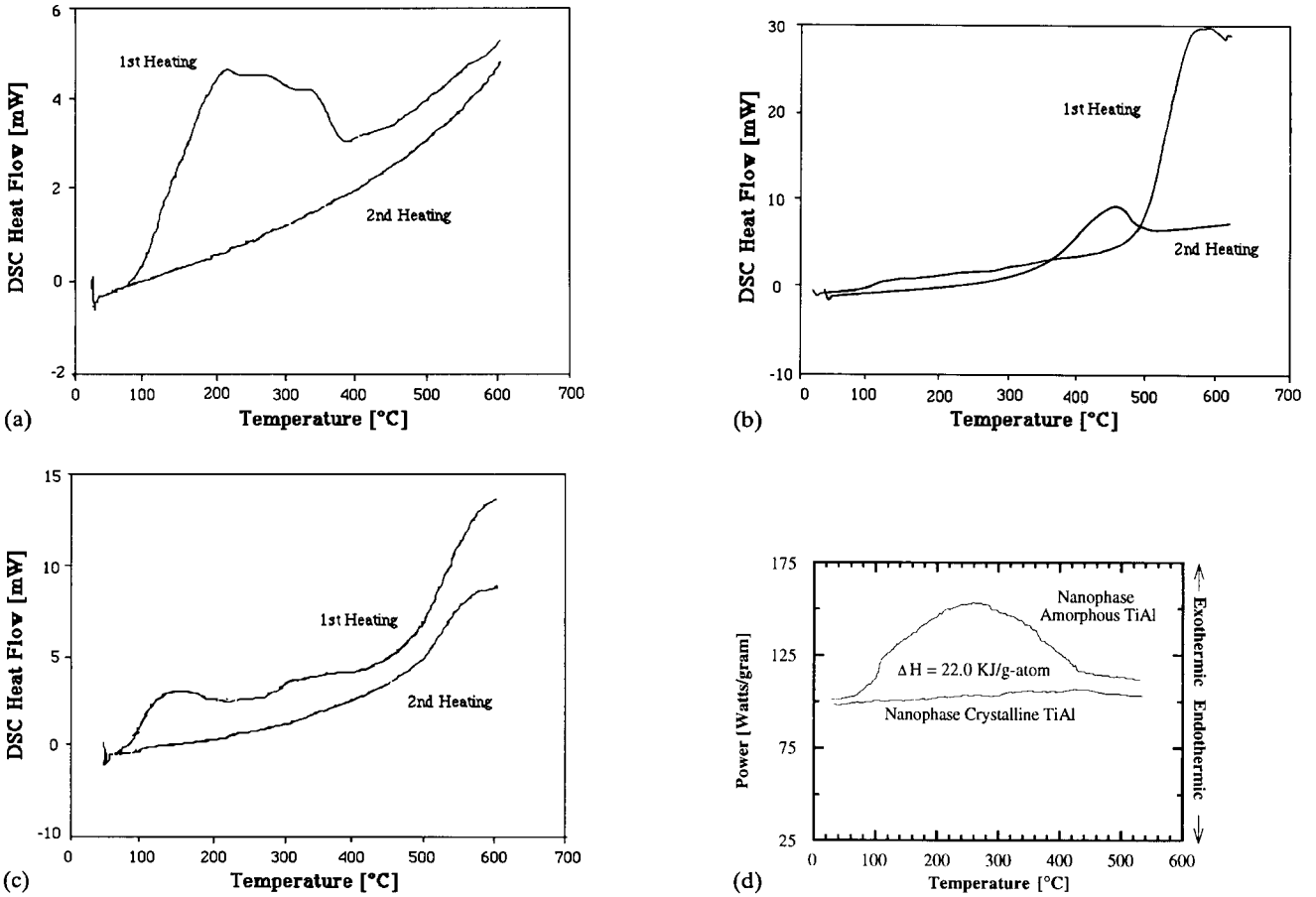

Fig. 3. DSC measurements on the alloys showing the heat evolution during the crystallization: (a) NiTi; (b) NiTb; (c) PdY; (d) TiAl.

of disorder and homogeneity are not known. However, noting that the heat of mixing in a regular solution model is given by, $\Delta H_{mix} = \Omega X_A X_B$, and that values of Ω in these systems are approximately 160 kJ mol^{-1} (the value for NiTi) a value of 5–10 kJ mol^{-1} seems possible, as was observed for the ordering of Ni_3Al [14]. These sources add to approximately 20–25 kJ mol^{-1} which is the magnitude of the heat release. Thus, the crystallization enthalpy appears to represent only a fraction of the total heat release; consequently, heat release measurements do not seem appropriate for investigating the amorphous to crystalline transition in nanophase alloys.

Finally, preliminary measurements of the density and Vickers hardness were performed on some of the samples. The results are summarized in Table 2. The densities of these samples, which were compacted at approximately 1 GPa in a WC powder press at the temperatures indicated in the table, were determined by gravimetry using Archimedes principle. The values of the relative density shown in the table refer to the ratio of the sample density to that of the intermetallic compound of Archimedes closest composition since the densities of the bulk amorphous alloys are not known.

TABLE 2. Vickers hardness and the density at different processing temperatures

Alloy	Density (g cm^{-3})	Relative density (%)	Hardness (GPa)	Compaction or sintering temperature (°C)
NiTi	5.7	87	3.5(±0.45)	150
	5.9	91	(not available)	200
NiTb	7.8	88	2.9(±0.32)	150
	8.4	94	4.5(±1.0)	200
	8.3	93	4.5(±1.0)	400[a]
PdY	6.2	–	2.7(±0.19)	RT
	6.3	–	3.1(±0.21)	200
TiAl	3.1	81	2.7(±0.18)	RT
	3.4	88	6.0(±0.07)	250[a]
	3.7	96	6.1(±0.05)	450[b]

[a]Partially crystalline.
[b]Mostly crystalline.

Most samples are 85%–95% dense. What fractions of this excess volume that can be attributed to pores grain boundaries or to the amorphous phase, itself, is difficult to estimate, although most samples showed no open porosity by Brunauer Emmet Toller (BET) measure-

ments. The high densities are reflected in the high values of the Vickers hardness, which range from 3 to 6 GPa. For comparison, we note that the Vickers hardness of the crystalline intermetallic γ-TiAl is approximately 3 GPa. Although the annealing treatments in this study are limited, it is observed that some densification can be affected by sintering, as noted by both the density and hardness measurements, without crystallization. The hardness of these materials seems comparable to that for nanocrystalline Pd which has a similar cohesive energy [15]. We believe that this result is a consequence of nanophase materials deforming by grain boundary sliding rather than by dislocation motion. Grain boundary sliding is unlikely to be sensitive to crystal structure or impurities.

4. Conclusions

This work demonstrates that nanophase processing is a promising method for fabricating amorphous alloys. It was shown that several metal–metal amorphous alloys could be produced by this method and consolidated to high densities before the onset of crystallization. It was further shown that the enthalpy stored in these materials is much higher than in amorphous alloys produced by other means. This appears to be associated with interface or "grain" boundaries in the consolidated amorphous materials, although this preliminary work is not conclusive on this point. It should be interesting, for example, to measure the stored enthalpy remaining in samples annealed to temperatures just below the onset of crystallization. Vickers hardness measurements showed that these samples have high hardness, in fact values typical of intermetallic compounds. What remains to be shown, however, is what ductility these materials possess and whether deformation mechanisms involving grain boundaries, for example Coble creep or grain boundary sliding, are possible.

Acknowledgments

The authors are grateful to Professor C. J. Altstetter and Dr. H. J. Höfler for helpful comments and to Dr. K. Foster for conducting the DSC measurements. The research was supported by the National Science Foundation under grant DMR 90-22415. One of us (H.C.) is grateful to the Federation of Advanced Materials Industries at the U.I.U.C. and the College of Engineering for partial support.

References

1 R. B. Schwarz and W. L. Johnson, *Phys. Rev. Lett., 51* (1983) 415.
2 E. Hellstern, H. J. Fecht, Z. Fu and W. L. Johnson, *J. Appl. Phys., 65* (1989) 305.
3 M. Atzmon, K. Unruh and W. L. Johnson, *J. Appl. Phys., 58* (1985) 3865.
4 R. S. Averback and H. J. Höfler, in D. van Aken, G. Was and A. Ghosh (eds.), *Microcomposites and Nanocrystalline Materials*, 1991, p. 27.
5 H. Gleiter, in N. Hansen, A. Horsewell, T. Lefferes and H. Lilholt (eds.), *2nd Int. Symp. Metallurgy and Materials Science*, Risø Nat. Lab., Roskilde, Denmark, 1981, p. 15.
6 D. L. Johnson, *J. Am. Ceram. Soc., 73* (1990) 2576.
7 H. Jing, A. Krämer, R. Birringer, H. Gleiter and U. Gonser, *J. Non-Cryst. Solids, 113* (1989) 167.
8 J. Weissmüller, R. Birringer and H. Gleiter, *Phys. Lett. A, 145* (1990) 130.
9 R. S. Averback, H. J. Höfler, H. Hahn and J. C. Logas, *Appl. Phys. Lett., 57* (1990) 1745.
10 R. Birringer, H. Gleiter, H. P. Klein and P. Marquardt, *Phys. Lett. A, 102* (1984) 315.
11 S. Yatsuya, A. Yanagida, K. Yamauchi and K. Mihama, *J. Cryst. Growth, 70* (1984) 536.
12 C. N. J. Wagner, *J. Alloys Comp., 194* (1993) 295.
13 H. Chang, C. J. Altstetter and R. S. Averback, *J. Mater. Res.*, in press.
14 J. S. C. Jang and C. C. Koch, *J. Mater. Res., 5* (1990) 498.
15 A. H. Chokshi, A. Rosen, J. Karch and H. Gleiter, *Scr. Metall., 23* (1989) 1679.